Hydraulic jump analysis for a Bingham fluid

Zhou, Jian Guo; Shu, Jian Jun; Stansby, P. K.

2007

Zhou, J. G., Shu, J. J., & Stansby, P. K. (2007). Hydraulic jump analysis for a Bingham fluid. Journal of hydraulic research, 45(4), 555-562.

https://hdl.handle.net/10356/95296

https://doi.org/10.1080/00221686.2007.9521791

Hydraulic jump analysis for a Bingham fluid

J.G. ZHOU, School of Mechanical, Aerospace and Civil Engineering, University of Manchester, Manchester M60 1QD, UK
J.-J. SHU, Department of Mathematical Studies, University of Leeds, Leeds LS2 9JT, UK
P.K. STANSBY, School of Mechanical, Aerospace and Civil Engineering, University of Manchester, Manchester M60 1QD, UK

Abstract

A theoretical study of the hydraulic jump in a Bingham fluid is presented in this paper. Based on the approximation for lubrication theory, the formulae for conjugate depths, sequent bottom shear stress and critical depth are established. Due to the absence of an exact solution of the basic equations for conjugate depths, an analytical approximation has been developed. This formula is shown to provide good results, with a small error of less than 4%. The analytical results have revealed that the critical depth and the ratio of conjugate depths increase until the bottom shear stress reaches a certain value and decreases above that. Both the critical depth and the ratio of conjugate depths have maximum values where the critical flow or the jump is coupled between the effects of shear-free and shear regions. Reasonable agreement is achieved between the theoretical results and experimental data for conjugate and critical depths. The observation that the critical depth increases greatly when the dimensionless yield stress $\lambda \geqslant 0.1$ in the experiment provides further justification for the theoretical approach.

RÉSUMÉ

Une étude théorique du ressaut hydraulique dans un fluide de Bingham est présentée dans cet article. Les formules pour des profondeurs conjuguées, l'effort de cisaillement inférieur résultant et la profondeur critique sont établis en partant de l'approximation de la théorie de la lubrification,. En raison de l'absence d'une solution exacte des équations de base pour des profondeurs conjuguées, une solution analytique a été développée. On montre que cette formule donne de bons résultats, avec une petite erreur inférieure à 4%. Les résultats analytiques montrent que la profondeur critique et le rapport des profondeurs conjuguées augmentent jusqu'à ce que l'effort de cisaillement de fond atteigne une certaine valeur et puis diminuent au-delà. La profondeur critique et le rapport des profondeurs conjuguées ont des valeurs maximum quand l'écoulement critique ou le ressaut est couplé entre les effets des régions avec et sans cisaillement. Un accord raisonnable est réalisé entre les résultats théoriques et les données expérimentales pour des profondeurs conjuguées et critiques. L'observation que la profondeur critique augmente considérablement quand la contrainte sans dimensions $\lambda \geqslant 0.1$ dans l'expérience conforte l'approche théorique.

Keywords: Bingham fluid, hydraulic jump, non-Newtonian fluid, open channel flow.

1. Introduction

In almost five centuries since the hydraulic jump was described by Leonardo da Vinci, there have been a large number of papers on hydraulic jumps involving Newtonian fluids, motivated by scientific and technical reasons. This includes Bakhmeteff and Matzke (1936), Bidone (1820), Chow (1959), Rajaratnam (1967), Sarma and Newnham (1973), Watson (1964), U.S. Bureau of Reclamation (1955) and Task Force on Energy Dissipators for Spillways and Outlet Works of the Committee on Hydraulic Structures (1964). These studies permitted design charts to be prepared which were particularly useful for the design of small stilling basins. The hydraulic jump in non-Newtonian fluids has received considerably less attention yet is a necessary first step in gradually varied flow analysis.

The hydraulic jump is an important feature in the flow of mud over a dam. The mud, a mixture of water and cohesive clay particles, behaves as an inelastic non-Newtonian fluid. The reason for the inelastic non-Newtonian behaviour lies in the chemical cross-links between the clay particles. The cross-link formation resists motion as a solid until a yield stress is reached, at which point the cross-links are mechanically broken and the mud behaves as a fluid.

The Bingham fluid is a simple model which is widely used for this type of non-Newtonian fluid. In this model the process of the cross-link formation and destruction is instantaneous. Its thixotropic tendency has been ignored and the excess deviatoric stress τ over the yield stress τ_0 is assumed to be a linear function of the strain rate $\partial u/\partial y$, so that (see Fig. 1)

$$\mu_0 \frac{\partial u}{\partial y} = \begin{cases} 0 & \text{if } |\tau| < \tau_0 \\ \tau - \tau_0 \operatorname{sign}\left(\frac{\partial u}{\partial y}\right) & \text{if } |\tau| \geq \tau_0 \end{cases} \tag{1}$$

where μ_0 is the fluid viscosity. Note that for a Newtonian fluid $\tau_0 = 0$.

Our aim is to seek an adequate mathematical model for the hydraulic jump in a Bingham fluid to improve the prediction of prototype performance from physical models and to extend or interpret field or laboratory data with non-Newtonian properties.

Experiments on a hydraulic jump in a Bingham fluid have recently been conducted by Ogihara and Miyazawa (1994) using a mixture of water and bentonite which is regarded as a Bingham fluid. It was observed that the critical depth increased dramatically when the relative yield stress was over 0.1. This phenomenon is not amenable to any current theoretical analysis based on Newtonian fluid mechanics. In this paper, the macroscopic description of the jump is taken a step forward to describe such non-Newtonian behavior. Formulae for conjugate depths,

sequent bottom shear stress and critical depth are derived. Theoretical analysis is carried out and the solution to the basic equations is compared with experimental data.

2. Governing equations

A Bingham fluid is characterized by a yield stress. Only if the driving shear stress is larger than the yield stress, can it flow. Otherwise, the Bingham fluid behaves as a shear-free "solid". Since the shear stress decreases towards the channel top or pipe centre, the Bingham fluid becomes solid in the upper region of the channel or the centre of the pipe and remains fluid elsewhere, i.e. the Bingham fluid in a channel consists of two regions: the shear-free and shear regions. This is sketched in Fig. 2.

The governing equations for the steady flow of a Bingham fluid can be written in vector form as

$$\nabla \cdot \mathbf{V} = 0 \tag{2}$$

$$\rho(\mathbf{V} \cdot \nabla)\mathbf{V} = \mathbf{F} + \nabla \cdot \sigma \tag{3}$$

$$\sigma = -p\delta + \tau \tag{4}$$

where p is the pressure, ρ the density, **V** the velocity vector, **σ** the stress tensor, **τ** the shear stress tensor, **δ** the Kronecker delta, **F** the external force and **∇** the gradient operator.

If the Bingham fluid in an open channel is approximated as a two-dimensional half-Poiseuille flow with an imposed dimensional pressure gradient in the x direction (see Fig. 2), the analytical solution for velocity can be obtained by integrating Eqs (3) and (4) (Liu and Mei, 1989),

$$U(\xi) = \begin{cases} U_0 & 1-\lambda \le \xi \le 1 \\ U_0\left[1-\left(\frac{\xi+\lambda-1}{\lambda-1}\right)^2\right] & 0 \le \xi < 1-\lambda \end{cases} \tag{5}$$

where $\xi = y/h$, $\lambda = \tau_0/\tau_w$, U_0 is the shear-free velocity (Fig. 2) and τ_w, is the shear stress at the channel bottom.

In most situations, the vertical acceleration is small and can be neglected with little loss of accuracy. For this reason, Eq. (3) in the y direction can be simplified and be replaced by

$$p = \rho g(h - y) \tag{6}$$

which is commonly used to approximate the pressure profile in open channel flows.

3. Hydraulic jump

Conjugate depths, sequent bottom shear stress and critical depth are of primary importance in defining the characteristics of a hydraulic jump. The basic equations for these quantities can be established based on the integral continuity and momentum equations, combined with the properties of the Bingham fluid.

By referring to Fig. 3 and using subscripts 1 and 2 to designate quantities upstream and downstream of the jump, after applying the integral continuity equation, we have

$$q = \int_0^{h_1} U_1(y)\mathrm{d}y = \int_0^{h_2} U_2(y)\mathrm{d}y \tag{7}$$

where q is the discharge per unit width.

Substitution of Eq. (5) into the above equation leads to

$$\frac{1}{3}U_{01}h_1(2+\lambda_1) = \frac{1}{3}U_{02}h_2(2+\lambda_2) \tag{8}$$

Similarly, after the integral momentum equation is applied, the following equation is obtained

$$\int_0^{h_1} \rho(\mathbf{V_1}\cdot\mathbf{n})U_1\,\mathrm{d}y + \int_0^{h_2} \rho(\mathbf{V_2}\cdot\mathbf{n})U_2\,\mathrm{d}y = \int_0^{h_1} p_1\,\mathrm{d}y - \int_0^{h_2} p_2\,\mathrm{d}y \tag{9}$$

Incorporation of Eqs (5) and (6) into the above equation results in

$$\frac{8+7\lambda_2}{15}U_{02}^2h_2 - \frac{8+7\lambda_1}{15}U_{01}^2h_1 = \frac{g}{2}(h_1^2 - h_2^2) \tag{10}$$

Generally, the flow conditions upstream of the jump are known, i.e. U_{01}, h_1 and λ_1 are given. The two equations, Eqs (8) and (10), are obviously not sufficient to determine the three unknowns U_{02}, h_2 and λ_2. An additional equation must be provided. This comes from the definition of shear stress in the Bingham fluid. From the definition in Eq. (1), we obtain upstream of the jump,

$$\mu_0\frac{\partial U_1}{\partial y}\bigg|_{y=0} = (\tau_1 - \tau_0)|_{y=0} = (\tau_{w1} - \tau_0) \tag{11}$$

Substitution of Eq. (5) into the above equation leads to

$$\frac{2\mu_0 U_{01}}{h_1(1-\lambda_1)} = (\tau_{w1} - \tau_0) \tag{12}$$

Similarly, we have the following expression downstream of the jump as

$$\frac{2\mu_0 U_{02}}{h_2(1-\lambda_2)} = (\tau_{w2} - \tau_0) \tag{13}$$

Combining Eqs (12) and (13) results in

$$\frac{U_{01}h_2}{U_{02}h_1} = \frac{\lambda_2}{\lambda_1}\left(\frac{1-\lambda_1}{1-\lambda_2}\right)^2 \tag{14}$$

Equations (8), (10) and (14) are the basic equations for the three unknowns U_{02}, h_2 and λ_2 in the hydraulic jump for the Bingham fluid.

It should be noted that there are only two unknowns, U_{02}, h_2 for the hydraulic jump in a Newtonian fluid. Furthermore it is impossible to obtain an exact solution to the basic equations for the Bingham fluid, as will be shown in Section 3.1, except for the critical depth which will be described in Section 4.

3.1. Solution to the basic equations

A further mathematical consideration indicates that there is no exact solution to the basic equations and an asymptotic solution in one specific situation can be developed.

Substitution of Eq. (8) into Eq. (10) and Eq. (14), respectively, gives the following pair of equations

$$\frac{8+7\lambda_2}{\eta}\left(\frac{2+\lambda_1}{2+\lambda_2}\right)^2 - (8+7\lambda_1) = \frac{5(2+\lambda_1)^2}{6F_{r1}^2}(1-\eta^2) \tag{15}$$

$$\eta^2\frac{2+\lambda_2}{2+\lambda_1} = \frac{\lambda_2}{\lambda_1}\left(\frac{1-\lambda_1}{1-\lambda_2}\right)^2 \tag{16}$$

where $\eta = h_1/h_2$ and $F_{r1} = V_{01}/\sqrt{gh_1}$, is the Froude number, in which V_{01} is the depth-averaged velocity defined by

$$V_0 = \frac{1}{h}\int_0^h U(y)\mathrm{d}y = \frac{1}{3}U_0(2+\lambda) \tag{17}$$

Combining Eqs (15) and (16) will lead to a polynomial equation of fifth order in terms of either η or λ_2. According to algebraic field theory, there are no exact solutions. Numerical solutions will be discussed in Section 5.

The form of Eq. (15) suggests that an asymptotic solution can be derived in the case of $\eta \rightarrow 1$ as follows.

Defining

$$f(\lambda_2) = \frac{8+7\lambda_2}{(2+\lambda_2)^2} \tag{18}$$

Equation (15) becomes

$$\frac{f(\lambda_2)}{\eta}(2+\lambda_1)^2-(8+7\lambda_1)=\frac{5(2+\lambda_1)^2}{6F_{r1}^2}(1-\eta^2) \tag{19}$$

With reference to Eq. (16), $\lambda_2$is a function of η. Thus $f(\lambda_2)$ can be expanded in terms of $(1-\eta)$ by use of Taylor series

$$f(\lambda_2)=f(\lambda_2)|_{\eta\to 1}-\left.\frac{\mathrm{d}f(\lambda_2)}{\mathrm{d}\eta}\right|_{\eta\to 1}(1-\eta)+O(1-\eta)^2 \tag{20}$$

$\lambda_2 \to \lambda_1$ as $\eta \to 1$, hence

$$f(\lambda_2)|_{\eta\to 1}=f(\lambda_1) \tag{21}$$

According to the chain rule,

$$\frac{\mathrm{d}f(\lambda_2)}{\mathrm{d}\eta}=\frac{\mathrm{d}f(\lambda_2)}{\mathrm{d}\lambda_2}\frac{\mathrm{d}\lambda_2}{\mathrm{d}\eta} \tag{22}$$

and we have

$$\left.\frac{\mathrm{d}f(\lambda_2)}{\mathrm{d}\eta}\right|_{\eta\to 1}=-\frac{(2+7\lambda_1)(1-\lambda_1)\lambda_1}{(2+\lambda_1)^2(\lambda_1^2+\lambda_1+1)} \tag{23}$$

Substitution of Eqs (21) and (23) into Eq. (20) yields

$$f(\lambda_2)=\frac{8+7\lambda_1}{(2+\lambda_1)^2}+\frac{(2+7\lambda_1)(1-\lambda_1)\lambda_1}{(2+\lambda_1)^2(\lambda_1^2+\lambda_1+1)}\times(1-\eta)+O(1-\eta)^2 \tag{24}$$

Therefore, after substitution of Eq. (24) into Eq. (19) and rearrangement, we have

$$\frac{1}{\eta}\left[(8+7\lambda_1)(1-\eta)+\frac{(2+7\lambda_1)(1-\lambda_1)\lambda_1}{\lambda_1^2+\lambda_1+1}(1-\eta)+O(1-\eta)^2\right]=\frac{5(2+\lambda_1)^2}{6F_{r1}^2}(1-\eta^2) \tag{25}$$

This can further be simplified as

$$\eta(1+\eta)=\frac{6}{5}F_{r1}^2\frac{8+17\lambda_1+20\lambda_1^2}{(\lambda_1^2+\lambda_1+1)(2+\lambda_1)^2}[1+O(1-\eta)] \tag{26}$$

By ignoring terms of order $(1-\eta)$ and higher, Eq. (26) becomes a quadratic equation

$$\eta^2+\eta-2C_0F_{r1}^2=0 \tag{27}$$

Where

$$C_0=\frac{3}{5}\frac{8+17\lambda_1+20\lambda_1^2}{(\lambda_1^2+\lambda_1+1)(2+\lambda_1)^2} \tag{28}$$

The analytical solution to Eq. (27) is

$$\eta = \frac{1}{2}\left[\sqrt{1 + 8C_0 F_{r1}^2} - 1\right] \tag{29}$$

Equation (29) is the approximate formula for the conjugate depths. Theoretically, only under the condition that η is close to unity, can it be valid. However, the analysis and discussion in Sections 3.2 and 5.3 will indicate that it can also be used for other situations where η is larger than unity with a good accuracy.

After η is obtained through Eq. (29), U_{02} and λ_2 can be calculated by Eqs (8) and (16), respectively.

3.2. Analysis of the solution

The analysis of the solution of Eqs (15) and (16) based on a numerical method will be given in Section 5. Here we analyse and discuss the analytical solution (29).

The solution from Eq. (29) for the hydraulic jump in a Bingham fluid can be extended to two extreme cases: the solution for a hydraulic jump in fully-developed Newtonian viscous flow when λ_1 = 0 or C_0 = 6/5, and that in inviscid flow when λ_1= 1 or C_0 = 1. In the range 0 < λ_1 < 1, C_0 is a function of λ_1. Mathematical manipulation indicates that C_0 > 1 and there exists one maximum value of C_0 , that is C_{0max} = 1.22 when λ_1 = 0.213 or τ_0 /τ_{w1} = 0.213. C_0 increases with λ_1 when 0 $\leqslant\lambda_1\leqslant$ 0.213 and decreases with λ_1 when 0.213 < $\lambda_1\leqslant$ 1. This is shown graphically in Fig. 4 noting that $h_c/h_q = \sqrt[3]{C_0}$ which will be given in Eq. (32) below.

Thus, for the hydraulic jump in a Bingham fluid, the ratio of depths between downstream and upstream is always bigger than that in inviscid flow; it is also bigger than that in fully-developed Newtonian viscous flow when 0 $\leqslant\lambda_1\leqslant$ 0.41, but smaller when λ_1 is out of this range. The ratio of depths between downstream and upstream reaches the maximum when λ_1 = 0.213 as seen in Fig. 4. Gajjar and Smith (1983) analysed the process leading to a hydraulic jump in a uniform velocity layer with a thin sublayer at its bottom. They showed that the jump results from a viscous-inviscid interaction. For a fully-developed Bingham fluid in open channel, the flow in shear-free and shear regions can analogously be regarded as within "inviscid" and "viscous" layers respectively. The jump is strongly affected by this kind of viscous–inviscid interaction, so are the conjugate and the critical depths. Hence, this suggests that the maximum ratio of conjugate depths will appear when the jump is coupled between the effects of shear-free and shear regions, both of which have the same influence on the jump. When 0 $\leqslant\lambda_1\leqslant$ 0.213, the shear region dominates the jump and the relative jump height h_2 / h_1 increases as a function of λ_1; when 0.213 $\leqslant\lambda_1\leqslant$ 1, the shear-free region dominates the jump and h_2 / h_1 decreases as a function of λ_1 .

In order to give an insight into the behaviour of the sequent bottom shear stress τ_{w2} or λ_2, Eq. (16) can be rearranged as

$$\lambda_2^3 + r\lambda_2 + 2 = 0 \tag{30}$$

Where

$$r = -3 - \frac{(2+\lambda_1)(1-\lambda_1)^2}{\eta^2\lambda_1} \tag{31}$$

This is a standard cubic equation. It can easily be proved that its discriminant is always less than zero under the condition $0 < \lambda_1 < 1$. According to algebraic field theory, there are three different real roots: two are positive and one negative. But only one, which is larger than λ_1, is a possible solution. Thus, the bottom shear stress τ_{w2} downstream is always smaller than τ_{w1} upstream of the jump in a Bingham fluid, as for a Newtonian fluid.

4. Critical depth

When the depths upstream and downstream of the jump are the same, the flow is referred to as critical flow. Since the approximate formula (29) becomes an exact solution when $\eta = 1$, it can be used to derive a formula for critical depth.

By setting $\eta = 1$ and $h_2 = h_1 = h_c$ with $F_{r1} = q/\sqrt{gh_c^3}$, Eq. (29) results in

$$h_c = \sqrt[3]{C_0\frac{q^2}{g}} \tag{32}$$

where h_c is the critical depth and

$$C_0 = \frac{3}{5}\frac{8+17\lambda+20\lambda^2}{(\lambda^2+\lambda+1)(2+\lambda)^2} \tag{33}$$

with $\lambda = \tau_o/\tau_w$ due to $\lambda_1 = \lambda_2 = \lambda$ in critical flow.

Equation (32) is the formula for critical depth in a Bingham fluid. Clearly, it will be the solution for fully viscous flow if $\lambda = 0$ or $C_0 = 6/5$ and the one for fully inviscid flow if $\lambda = 1$ or $C_0 = 1$. h_c changes with λ in the interval $0 < \lambda < 1$. With reference to the nature of the function C_0 discussed in Section 3.2, it is evident that hc increases with λ when $0 \leqslant \lambda_1 \leqslant 0.213$ and decreases when $0.213 < \lambda \leqslant 1$. h_c reaches the maximum value of $1.068\sqrt[3]{q^2/g}$ at $\lambda = 0.213$, where the critical flow is coupled between the effects of the shear-free and shear regions. Furthermore, the shear region dominates the critical flow in the interval $0 \leqslant \lambda_1 \leqslant 0.213$ and the shear-free region dominates the flow in the interval $0.213 < \lambda \leqslant 1$. The features are also shown in Fig. 4 in terms of h_c/h_q against τ_o/τ_w or λ, where $h_q = \sqrt[3]{q^2/g}$. The critical depth is always greater than that

in fully inviscid flow, and it is also bigger than that in fully viscous flow when $0 \leqslant \lambda \leqslant 0.41$, but smaller when $0.41 < \lambda \leqslant 1$.

5. Numerical solution of the jump equation

As pointed out in Section 3.1, Eqs (15) and (16) cannot be solved exactly. Hence a numerical method is used to approach them. In the present study, Newton's method is applied to obtain the numerical solution.

5.1. Conjugate depths

The numerical results for the conjugate depths are plotted in Figs 5 and 6. It is clearly seen that η or h_2/h_1 is almost a linear function of F_{r1} but is not a linear function of τ_o/τ_{w1} or λ_1. η always increases with F_{r1} but it may increase or decrease depending on the value of λ_1, which can clearly be viewed from the figures. As expected, there is one peak or maximum value of η when λ_1 changes from 0 to 1.

5.2. Sequent bottom shear stress

Since $\lambda_2 = \tau_0 = \tau_{w2}$, λ_2 represents the feature of the sequent bottom shear stress. The numerical dependence of λ_2 against λ_1 is shown in Fig. 7. As analysed in Section 3.2, λ_2 is always greater than λ_1 and increases as a function of λ_1. The difference between the bottom shear stresses upstream and downstream of the jump increases with F_{r1} and vanishes at $\lambda_1 = 0$ or 1 when $\lambda_2 = 0$ or 1, i.e. $\tau_{w2} = \tau_{w1}$.

5.3. Comparison of numerical results and analytical solution

In Section 3.1, the analytical solution for conjugate depths is derived for η close to unity. In order to examine its accuracy, a comparison between the numerical results of Eqs (15) and (16) and the analytical solution of Eq. (29) is carried out. The results are plotted in Figs 8–11.

Figure 8 shows that the difference between the results increases significantly with F_{r1}. Figure 9 reveals that η for the two results reaches a maximum at the different values of τ_o/τ_{w1} or λ_1. Since the critical depth reaches a maximum at the same λ_1 ($\lambda_1 = \lambda$ for critical flow) as the conjugate depths from the analytical solution (29) (see Sections 3.2 and 4), the conjugate depth η from the numerical results and the critical depth h_c do not reach their maximum at the same value of λ_1. This indicates that different λ_1 is required, respectively, for the hydraulic jump and for the critical flow to be coupled between shear-free and shear regions. λ_1 for the former is smaller than that for the latter, hence at smaller λ_1 the jump is coupled between the two regions,

whereas at bigger values the critical flow is coupled. Also, the biggest difference from the two solutions takes place in the vicinity of $\lambda_1 = 0.5$. Figure 10 further shows the significant increase in the difference between the results with F_{r1} when $|\lambda_1 - 0.5| < 0.1$. However, even for η larger than unity, the two results are still close to each other if $|\lambda_1 - 0.5| > 0.1$. Inparticular, when$\lambda_1 < 0.1$ or $\lambda_1 > 0.9$, they become almost identical. This is due to the assumption of $\lambda_2 \rightarrow \lambda_1$ introduced in Eq. (29) as $\eta \rightarrow 1$. Figure 11 shows that the relative error changes with τ_o / τ_{w1} as well as Fr1. The relative error is defined by $(\eta_{ana} - \eta_{num})/\eta_{num}$, where η_{num} is calculated from Eqs (15) and (16) by the numerical method with ηana from Eq. (29). It is clear that the relative errors are notably increased with Fr1 when $F_{r1} > 10$. For most values of τ_o / τ_{w1}, the analytical solution from Eq. (29) is larger than the numerical one from Eqs (15) and (16). In addition, the relative error increases with λ_1 until it is above a certain value which is a function of F_{r1} and then decreases to zero after that. The computation has shown that the relative error is smaller than 4% in the test range of $F_{r1} \leqslant 25$. Therefore Eq. (29) is a reasonable approximate formula for conjugate depths. If $|\lambda_1 - 0.5| > 0.1$, even in the situation where η is much greater than unity, an accurate result is obtained.

6. Verification of the formulae

Ogihara and Miyazawa (1994) carried out an experimental investigation into the hydraulic jump in a Bingham fluid using a mixture of water and bentonite. Such a mixture can normally be treated as a Bingham fluid based on its flow characteristics. Their experimental results are used to validate the theoretical results in the present study.

6.1. Conjugate depths

The comparison between the theoretical results and the experimental data for conjugate depths is plotted in Fig. 12. The experimental data are directly adopted from the results by Ogihara and Miyazawa, and the theoretical values are numerically calculated from Eqs (15) and (16). It can be seen that the experimental data are scattered. This may be due to the difficulty in measuring the conjugate depths. Nevertheless the magnitudes are quite similar.

6.2. Critical depth

Figure 13 shows that the exact solution (32) of critical depth as a function of discharge is in satisfactory agreement with Ogihara and Miyazawa's experimental data.

In addition, Ogihara and Miyazawa reported that the critical depth increased dramatically when the dimensionless yield stress λ exceeded 0.1 in the experiment. This supports the theoretical result from the present study because h_c increases with λ in the range of $0 \leqslant \lambda \leqslant$

0.213. As indicated in Section 4, the critical depth continues to increase up to λ = 0.213. After that, it decreases with λ. Unfortunately, in the experiment, there are no further results available for this comparison.

7. Conclusions

The hydraulic jump in a Bingham fluid has been investigated, based on the approximation for lubrication theory. Formulae for conjugate depths, sequent bottom shear stress and critical depth are derived. The critical depth reaches a maximum at λ = 0.213 where the critical flow is coupled between the effects of shear-free and shear regions. The sequent bottom shear stress τ_{w2} is always smaller than τ_{w1}, i.e. $\tau_{w2} < \tau_{w1}$ or $\lambda_2 > \lambda_1$. When λ_1 = 0 or 1, the solution is consistent with fully viscous or fully inviscid flows. In addition, an analytical solution for conjugate depths is developed for η close to unity. Study of the results from the analytical and numerical solutions suggests that this formula can also be valid in the situation where η is much larger than unity as long as $|\lambda_1 - 0.5| > 0.1$. The error caused by the approximation is always less than 4%. Validation of the formulae is carried out by comparison between the theoretical results and Ogihara and Miyazawa's experimental data. The analysis indicates that satisfactory agreement is achieved for both conjugate and critical depths. The formula also indicates that there is an apparent increase of critical depth when $\tau_0 / \tau_w \leqslant 0.213$, which has been supported by the experimental observation that critical depth increased greatly as $\tau_0 / \tau_w \geqslant 0.1$.

References

1. BAKHMETEFF, B.A. and MATZKE, A.E. (1936). "The Hydraulic Jump in Terms of Dynamic Similarity". *Trans. Am. Soc. Civil Eng.* 101(1935), 630–680.

2. BIDONE, G. (1820). "Expérience sur le Remous et la Propagation des Ondes". *Memorie della Reale Accademia delle Scienze di Torino, Turin* 25, 21–112 (in Italian).

3. CHOW, V.T. (1959). *Open-channel Hydraulics*. McGraw-Hill Book Company, New York.

4. GAJJAR, J.S.B. and SMITH, F.T. (1983). "On Hypersonic Self-induced Separation, Hydraulic Jumps and Boundary Layers with Algebraic Growth". *Mathematika* 30, 77–93.

5. LIu, K.F. and MEI, C.C. (1989). "Slow Spreading of a Sheet of Bingham Fluid on an Inclined Plane". *J. Fluid Mech.* 207, 505–529.

6. OGIHARA, Y. and MIYAZAWA, N. (1994). "Hydraulic Characteristics of Flow over Dam and Hydraulic Jump of Bingham Fluid". *Proc. Jpn. Soc. Civil Eng.* 485(2–26), 21–26 (in Japanese).

7. RAJARATNAM, N. (1967). '*Hydraulic Jumps'*, *Vol. 4 of Advances in Hydroscience*. Academic Press, NewYork, NY, pp. 198–280.

8. SARMA, K.V.N. and NEWNHAM, D.A. (1973). "Surface Pro-files of Hydraulic Jump for Froude Number less than Four". *Water Power* 25, 139–142.

9. Task Force on Energy Dissipators for Spillways and Outlet Works of the Committee on Hydraulic Structures (1964). "Energy Dissipators for Spillways and Outlet Works". *J. Hydraul. Div. Proc. Am. Soc. Civil Eng.* 90(HY1–3762), 121–147.

10. U.S. Bureau of Reclamation (1955). "Research Studies on Stilling Basins, Energy Dissipators and Associated Appurtenances". Technical Report No. Hyd–399, Denver, Colorado.

11. Watson, E.J. (1964). "The Radial Spread of a Liquid Jet Over a Horizontal Plane". *J. Fluid Mech.* 20(3), 481–499.

List of Figures

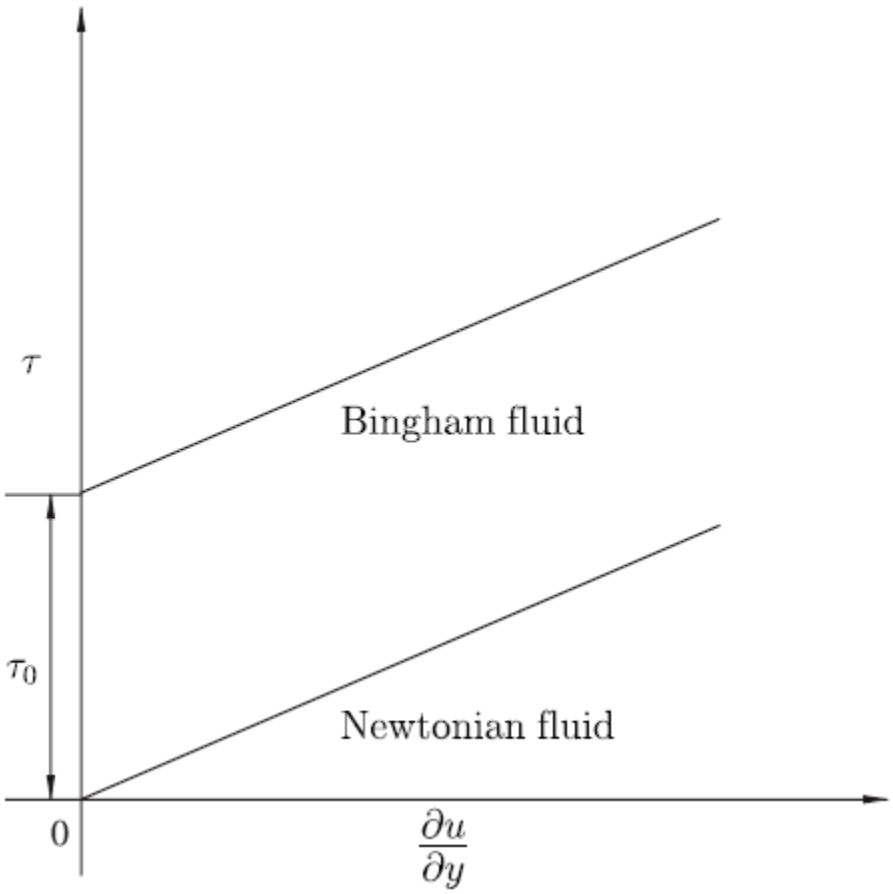
τ
Bingham fluid
τ_0
Newtonian fluid
0
$\frac{\partial u}{\partial y}$

Fig. 1

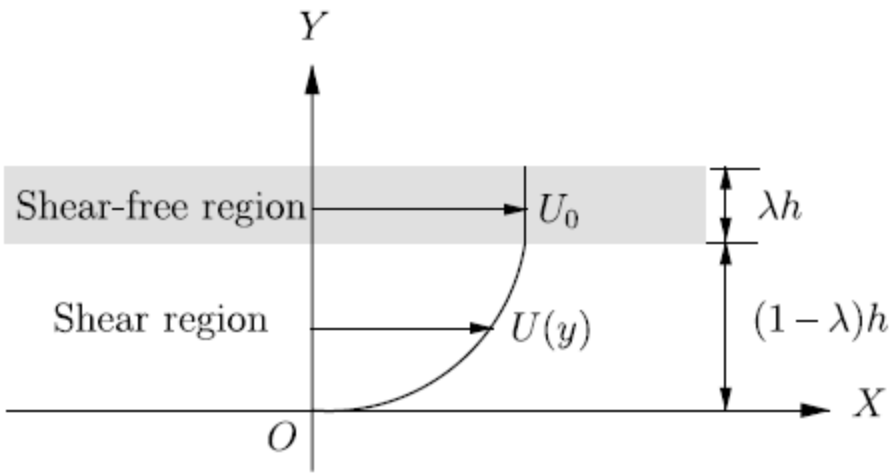

Fig. 2

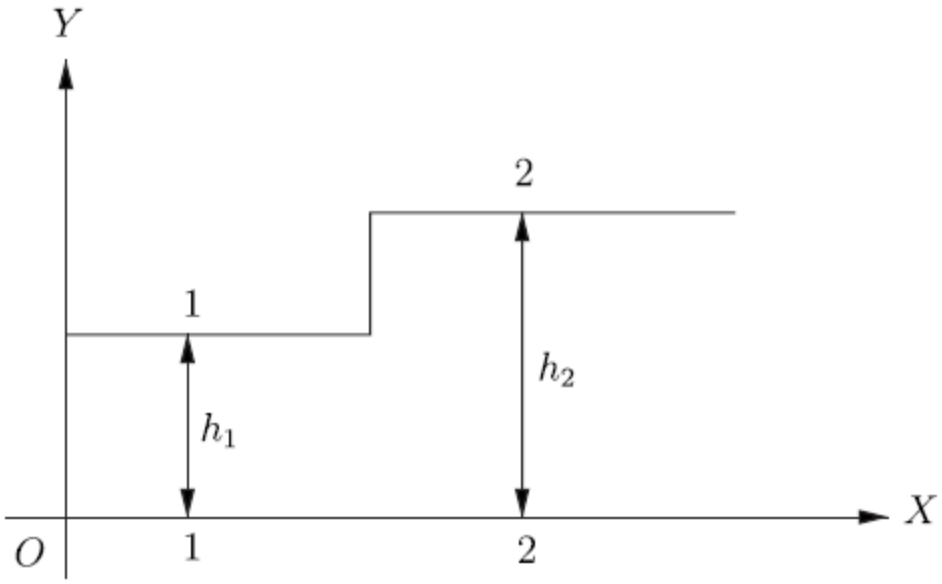

Fig. 3

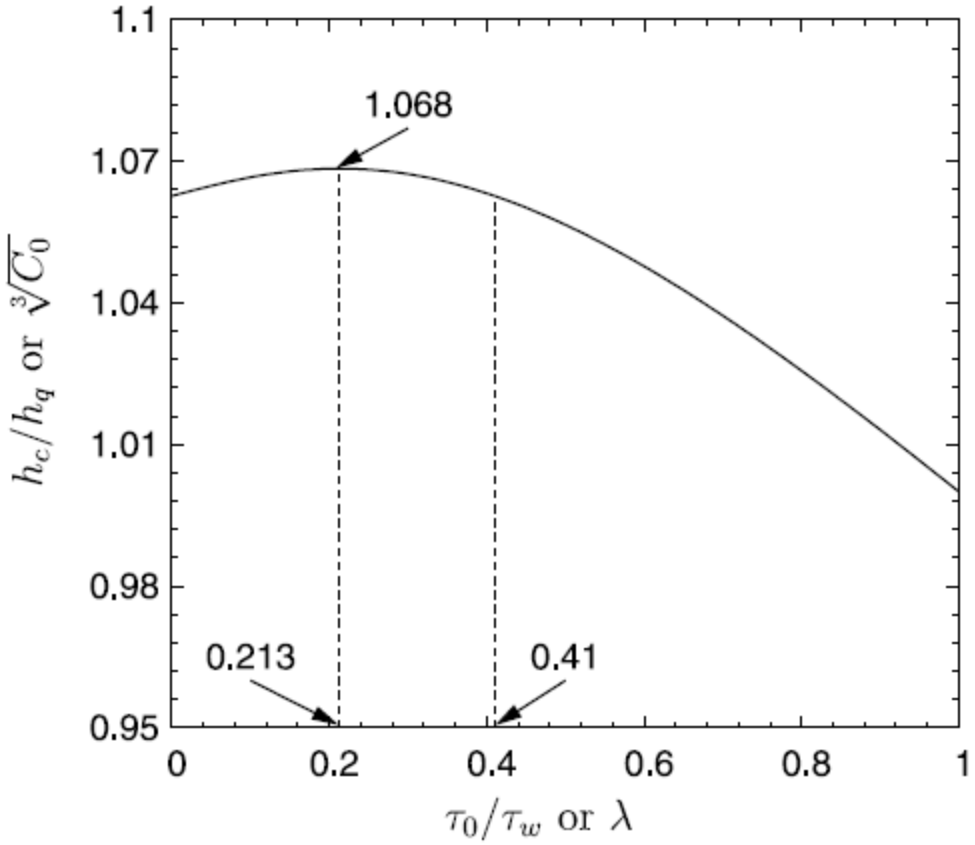
1.1
1.07
1.04
1.01
0.98
0.95
1.068
0.213
0.41
0
0.2
0.4
0.6
0.8
1
h_c/h_q or $\sqrt[3]{C_0}$
τ_0/τ_w or λ

Fig. 4

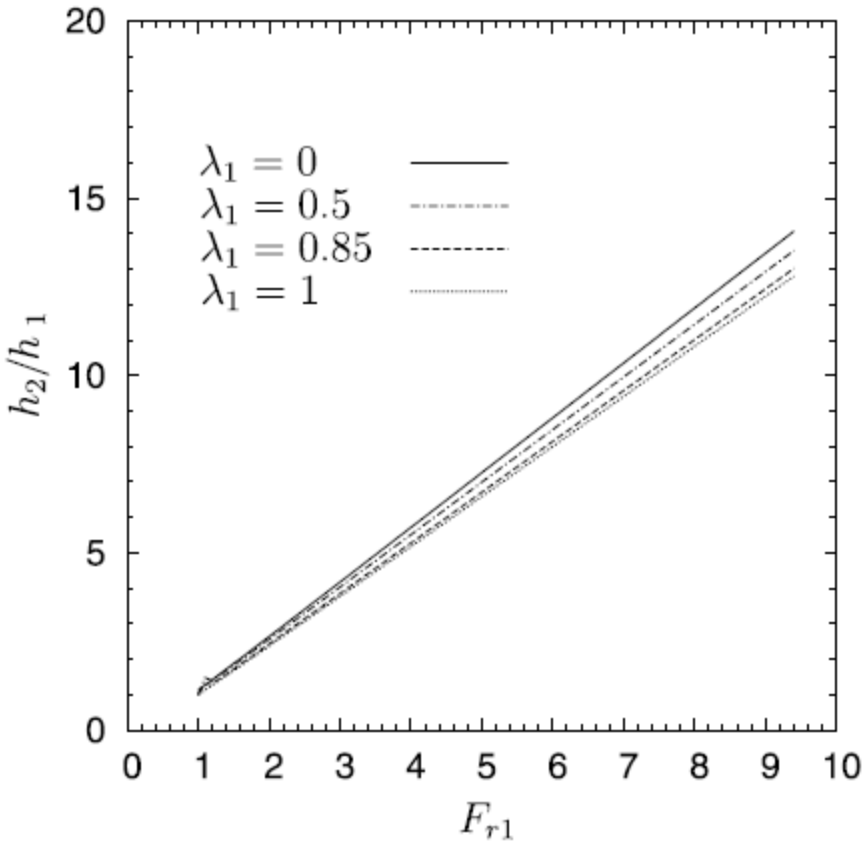
20
15
10
5
0
0
1
2
3
4
5
6
7
8
9
10
h_2/h_1
F_{r1}
$\lambda_1 = 0$
$\lambda_1 = 0.5$
$\lambda_1 = 0.85$
$\lambda_1 = 1$

Fig. 5

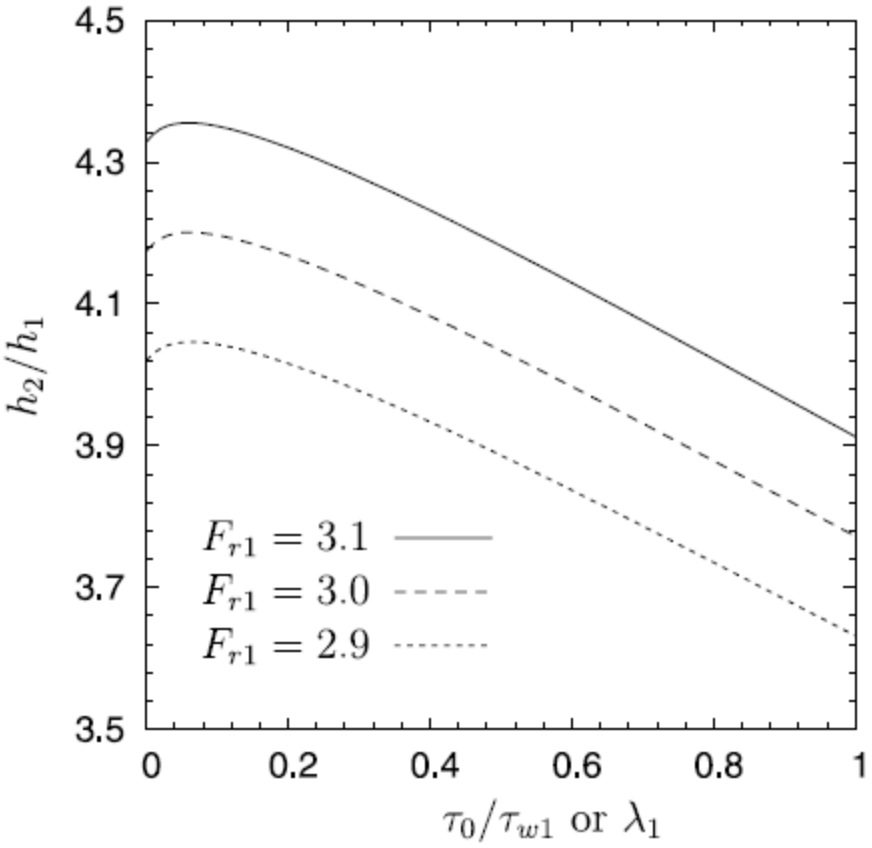
4.5
4.3
4.1
3.9
3.7
3.5
h_2/h_1
0
0.2
0.4
0.6
0.8
1
τ_0/τ_{w1} or λ_1
$F_{r1} = 3.1$
$F_{r1} = 3.0$
$F_{r1} = 2.9$

Fig. 6

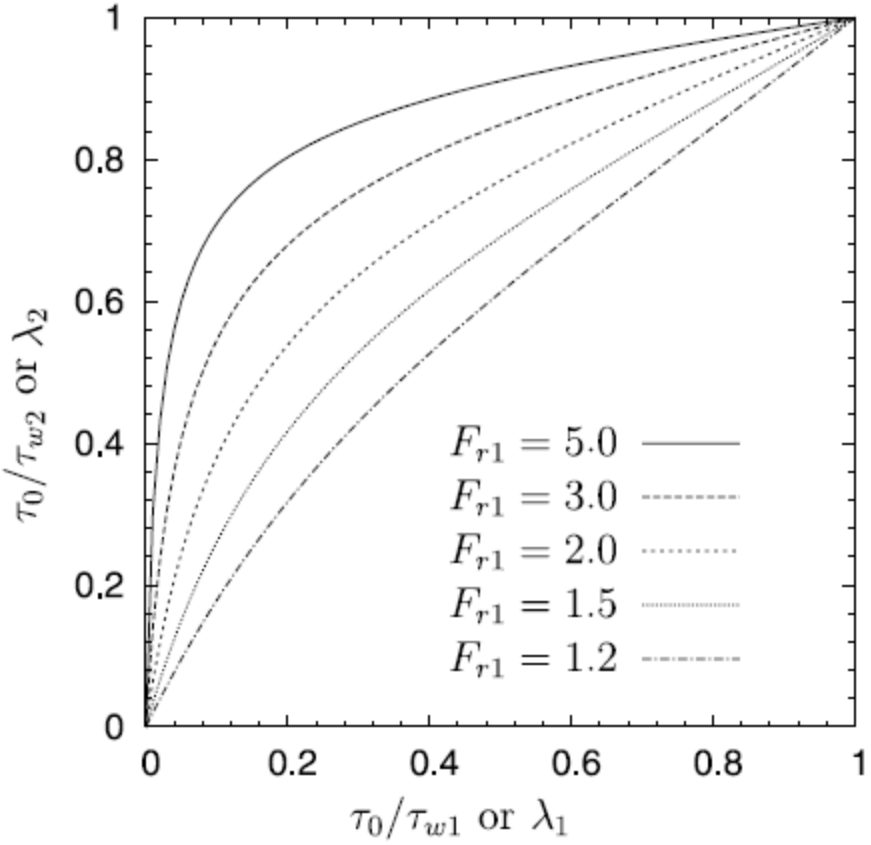
1
0.8
0.6
0.4
0.2
0
0
0.2
0.4
0.6
0.8
1
τ_0/τ_{w2} or λ_2
τ_0/τ_{w1} or λ_1
$F_{r1} = 5.0$
$F_{r1} = 3.0$
$F_{r1} = 2.0$
$F_{r1} = 1.5$
$F_{r1} = 1.2$

Fig. 7

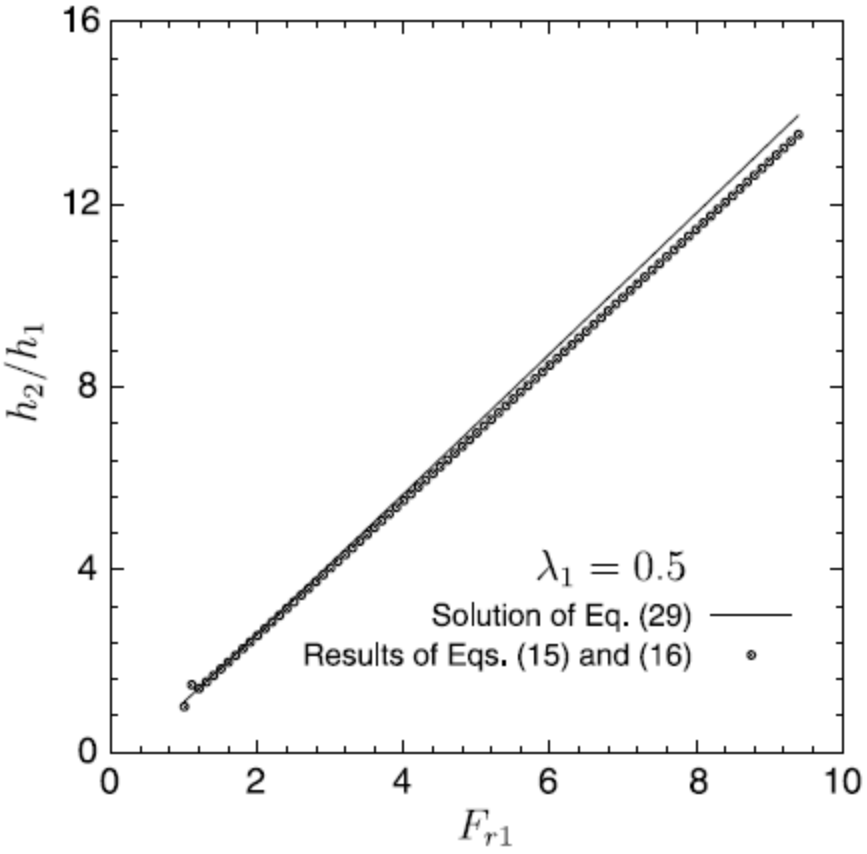
16
12
8
4
0
0
2
4
6
8
10
h_2/h_1
F_{r1}
$\lambda_1 = 0.5$
Solution of Eq. (29)
Results of Eqs. (15) and (16)

Fig. 8

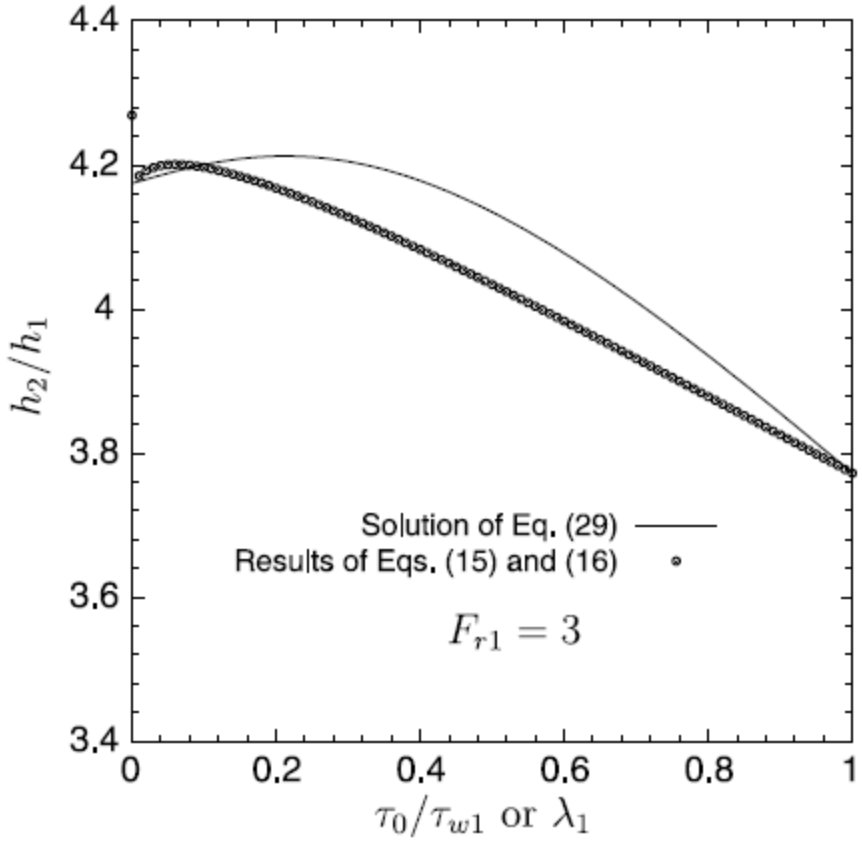
4.4
4.2
4
3.8
3.6
3.4
0
0.2
0.4
0.6
0.8
1
h_2/h_1
τ_0/τ_{w1} or λ_1
Solution of Eq. (29)
Results of Eqs. (15) and (16)
$F_{r1} = 3$

Fig. 9

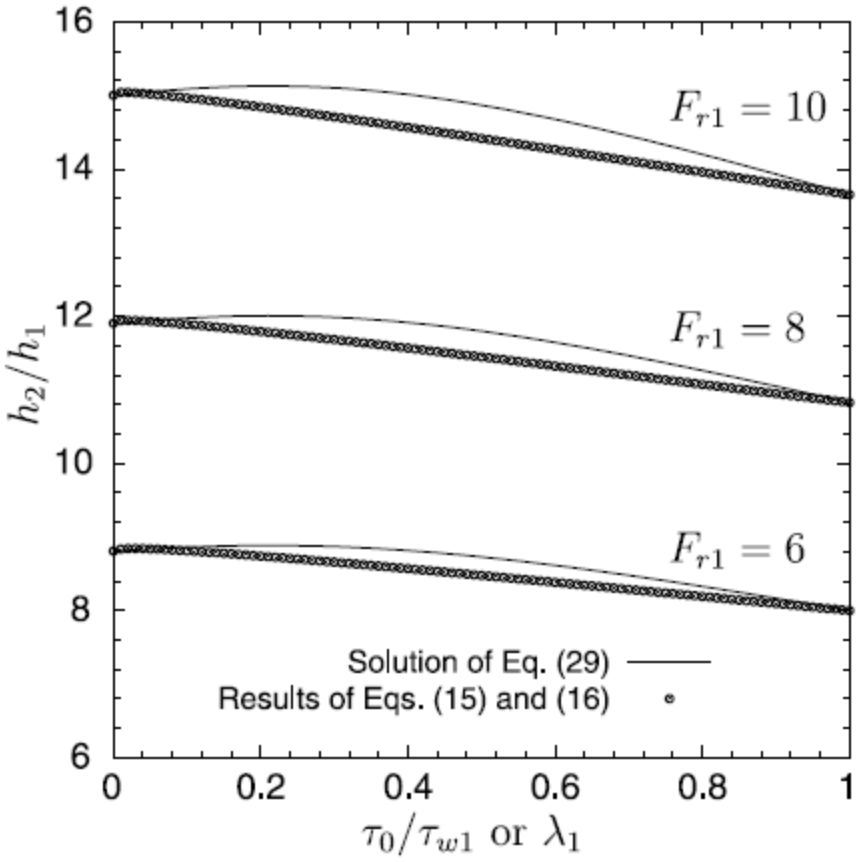
16
14
12
10
8
6
0
0.2
0.4
0.6
0.8
1
h_2/h_1
τ_0/τ_{w1} or λ_1
$F_{r1} = 10$
$F_{r1} = 8$
$F_{r1} = 6$
Solution of Eq. (29)
Results of Eqs. (15) and (16)

Fig. 10

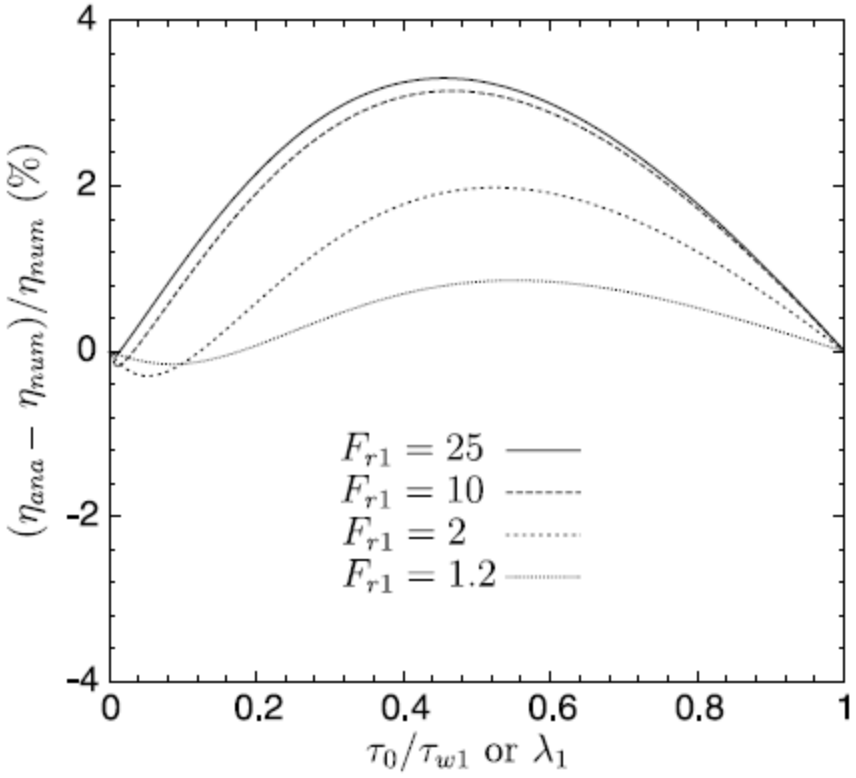
4
2
0
-2
-4
0
0.2
0.4
0.6
0.8
1
$(\eta_{ana} - \eta_{num})/\eta_{num}$ (%)
τ_0/τ_{w1} or λ_1
$F_{r1} = 25$
$F_{r1} = 10$
$F_{r1} = 2$
$F_{r1} = 1.2$

Fig. 11

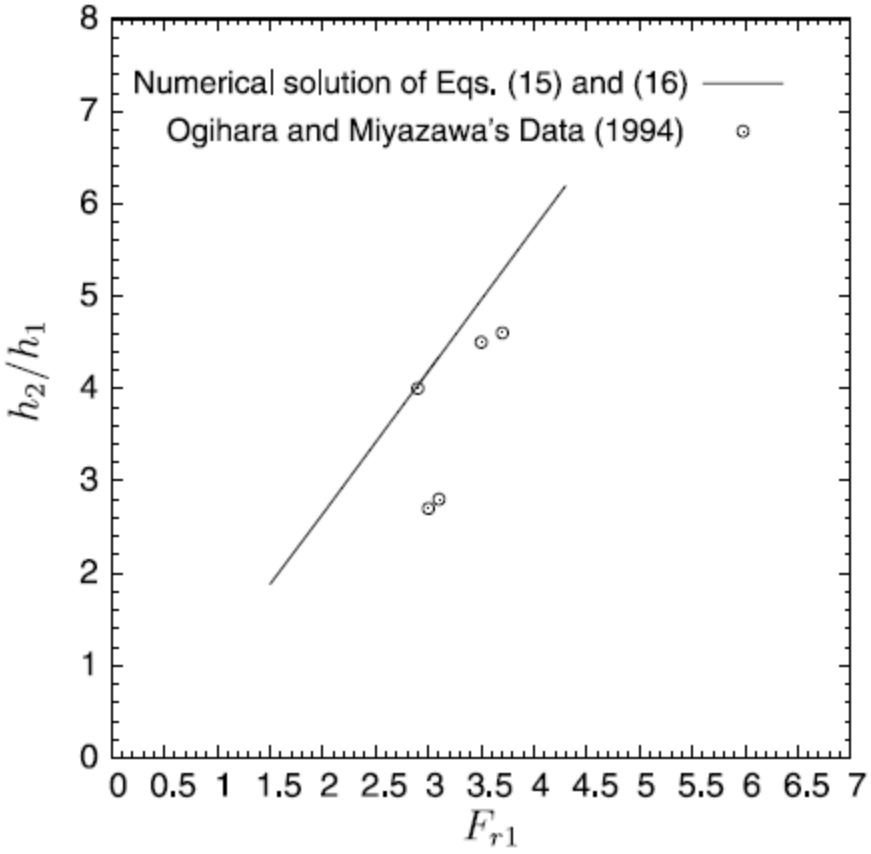
Numerical solution of Eqs. (15) and (16)
Ogihara and Miyazawa's Data (1994)
h_2/h_1
F_{r1}
0
1
2
3
4
5
6
7
8
0 0.5 1 1.5 2 2.5 3 3.5 4 4.5 5 5.5 6 6.5 7

Fig. 12

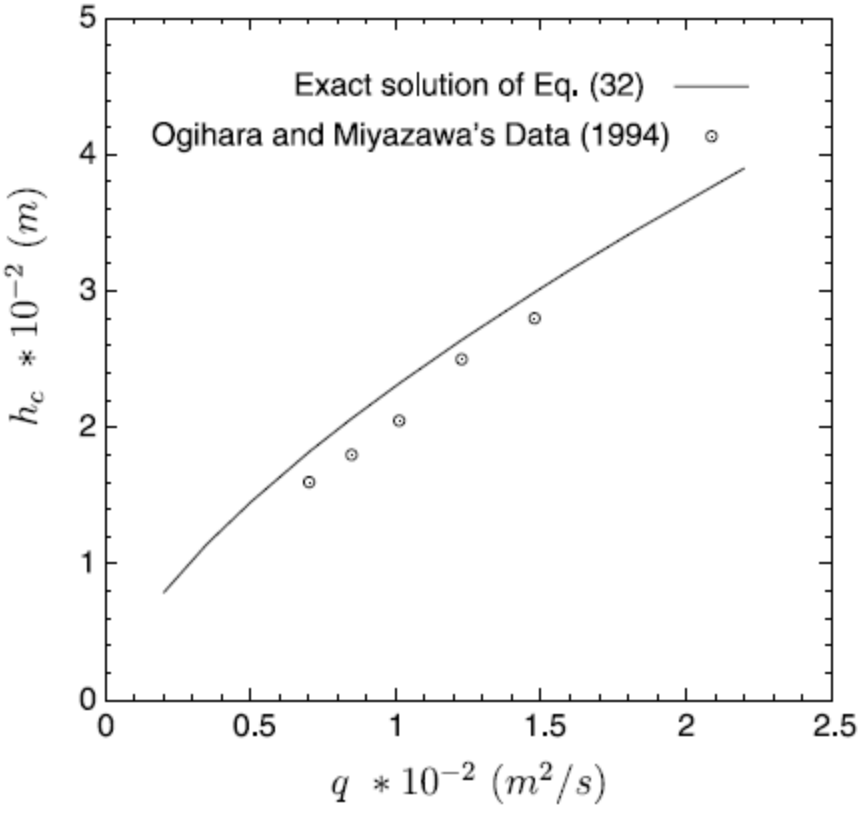
Exact solution of Eq. (32)
Ogihara and Miyazawa's Data (1994)
$h_c * 10^{-2}\ (m)$
$q * 10^{-2}\ (m^2/s)$
0
1
2
3
4
5
0
0.5
1
1.5
2
2.5

Fig. 13